SECURITY CLASSIFICATION OF THIS PAGE

REPORT DOCUMENTATION PAGE

Form Approved
OMB No. 0704-0188

1b. RESTRICTIVE MARKINGS

AD-A215 167

3. DISTRIBUTION/AVAILABILITY OF REPORT
Approved for public release; distribution unlimited.

(2)

4. PERFORMING ORGANIZATION REPORT NUMBER(S)

5. MONITORING ORGANIZATION REPORT NUMBER(S)
AFOSR-TR-89-1490

6a. NAME OF PERFORMING ORGANIZATION	6b. OFFICE SYMBOL (If applicable)	7a. NAME OF MONITORING ORGANIZATION
Michigan State University Electrical and Mechanical		AFOSR

6c. ADDRESS (City, State, and ZIP Code)	7b. ADDRESS (City, State, and ZIP Code)
Engineering Dept East Lansing, Mich 48824	BLDG 410 BAFB DC 20332-6448

8a. NAME OF FUNDING/SPONSORING ORGANIZATION	8b. OFFICE SYMBOL (If applicable)	9 PROCUREMENT INSTRUMENT IDENTIFICATION NUMBER
AFOSR		AFOSR-75-2842

8c. ADDRESS (City, State, and ZIP Code)	10 SOURCE OF FUNDING NUMBERS			
	PROGRAM ELEMENT NO.	PROJECT NO.	TASK NO	WORK UNIT ACCESSION NO.
BLDG 410 BAFB DC 20332-6448	61102F	2303	B1	

11. TITLE (Include Security Classification)
A STATISTICAL MODEL FOR HYDROGEN HALIDE PRODUCT DISTRIBUTIONS USING INFORMATION THEORY

12. PERSONAL AUTHOR(S)
D.H. Stone and R.L. Kerber

13a. TYPE OF REPORT	13b. TIME COVERED	14. DATE OF REPORT (Year, Month, Day)	15. PAGE COUNT
Final	FROM _____ TO _____	January 1980	41

16. SUPPLEMENTARY NOTATION

17. COSATI CODES			18. SUBJECT TERMS (Continue on reverse if necessary and identify by block number)
FIELD	GROUP	SUB-GROUP	

19. ABSTRACT (Continue on reverse if necessary and identify by block number)

20. DISTRIBUTION/AVAILABILITY OF ABSTRACT	21 ABSTRACT SECURITY CLASSIFICATION
☒ UNCLASSIFIED/UNLIMITED ☐ SAME AS RPT ☐ DTIC USERS	unclassified

22a NAME OF RESPONSIBLE INDIVIDUAL	22b TELEPHONE (Include Area Code)	22c OFFICE SYMBOL
	767-4960	NC

DD Form 1473, JUN 86 — Previous editions are obsolete. — SECURITY CLASSIFICATION OF THIS PAGE

A Statistical Model for Hydrogen Halide Product Distributions Using Information Theory*

D. H. Stone and R. L. Kerber
Michigan State University
East Lansing, MI 48824

Chemical laser modeling is dependent on the reaction rate coefficients available from both experiment and theory. A statistical model has been developed to correlate the relative rate coefficients for the laser pumping reactions:
(I) $F + H_2 \rightarrow HF(v,J) + H$, (II) $F + D_2 \rightarrow DF(v,J) + D$,
(III) $H + F_2 \rightarrow HF(v,J) + F$, (IV) $D + F_2 \rightarrow DF(v,J) + F$,
(V) $H + Cl_2 \rightarrow HCl(v,J) + Cl$, (VI) $D + Cl_2 \rightarrow DCl(v,J) + Cl$,
(VII) $H + Br_2 \rightarrow HBr(v,J) + Br$, and (VIII) $D + Br_2 \rightarrow DBr(v,J) + Br$.
The detailed product distributions for Reactions (IV) and (VIII) are generated by the model; these distributions have not yet been experimentally determined. The model uses surprisal analysis to relate the product rotational distributions for each reaction by considering each vibrational level separately. Using Polanyi's experimental data with RRHO prior rates results in rotational surprisals which are approximately quadratic in form and vary in width with vibrational level. A model was developed and applied to Reactions (III) and (VII) which assumes a reaction complex interaction among the product vibrational levels. An adjusted number of product states made available to each level by the interaction is then computed. The logarithm of this number is related to the width (or entropy) of each rotational surprisal distribution and a correlation is observed. The model also predicts the degree to which the surprisals skew toward high rotational levels. The model results coupled with the observed vibrational distributions favorably reproduce the rotational distributions for Reactions (III) and (VII). Assuming an isotopic independence for some parameters between Reactions (III) and (IV) and between (VII) and (VIII), the model can generate the full vibrotational distributions for (IV) and (VIII) from a small set of input parameters.

*This work was supported by AFOSR Grant No. 75-2842 and NSF Grant No. ENG 76-00733.

I. INTRODUCTION

Chemical laser modeling is dependent on the reaction rate coefficients available from both experiment and theory. A comprehensive computer model must incorporate potentially hundreds of rates for the various pumping and relaxation mechanisms, in order to accurately predict laser performance. Available reaction rate data for HF chemical lasers is taken from selected experiments and trajectory calculations as reviewed by Cohen and Bott in references 1 and 2. Not all reaction rates of interest in the HF laser have been studied and significant uncertainties are present in many that are known. Techniques are needed to expand the data base from a few accurately measured reaction rates to a complete rate set. In this paper, we apply the information - theoretic or "surprisal" approach to reaction product distributions as developed by Bernstein, Levine, and Ben-Shaul (references 3-5) to the experimental distributions obtained by Polanyi, Woodall, and Sloan (references 6-7) for the pumping reactions

$$F + H_2 \rightarrow HF(v,J) + H \qquad (I)$$

$$F + D_2 \rightarrow DF(v,J) + D \qquad (II)$$

$$H + F_2 \rightarrow HF(v,J) + F \qquad (III)$$

Our objectives are to develop a model which correlates the vibrotational product distributions for these reactions in order to describe the distributions in terms of a small set of parameters, and to predict the full vibrotational distribution for the reaction

$$D + F_2 \rightarrow DF(v,J) + F \qquad (IV)$$

We also apply the model to the experimental distributions obtained by Anlauf, et. al, (reference 8) for the reactions

$$H + Cl_2 \rightarrow HCl(v,J) + Cl \qquad (V)$$

$$D + Cl_2 \rightarrow DCl(v,J) + Cl \qquad (VI)$$

$$H + BR_2 \rightarrow HBr(v,J) + Br \qquad (VII)$$

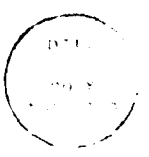

The model is then used to predict the product distribution for

$$D + Br_2 \rightarrow DBr(v,J) + Br \qquad \text{(VIII)}$$

This reaction product distribution has also not been studied experimentally.

The model incorporates well-documented reaction complex dynamics characteristic of Reactions (I)-(VIII) along with ideas similar to statistical collision theory as reviewed in reference 9. The surprisal technique is used to make the product distributions more tractable. We now review the surprisal approach and apply it to each reaction.

II. INFORMATION CONTENT OF AN EXPERIMENTAL DISTRIBUTION

From the development in reference 5 we consider the distribution of outcomes in an experiment which consists of a large number of repetitions, N, of the same event, with n possible outcomes. The probability of the ith outcome is defined as $P_i = N_i/N$, the fraction of times that we observe the ith outcome. The information content of the distribution is then given as:

$$I = \sum_i P_i \ln \frac{P_i}{1/n} \qquad (1)$$

The information attains its smallest value (zero) when $P_i = 1/n$ so that all the possible outcomes arise with equal probability.

The entropy of the distribution is defined by

$$H = -\sum_i P_i \ln P_i \qquad (2)$$

where the thermodynamic entropy $S = RH$, and R is the gas constant. Then

$$I = \ln(n) - H \qquad (3)$$

Both the information and entropy are nonnegative numbers.

The prior distribution, P^o, of product states (outcomes) is given as the one which corresponds to $I = 0$. Thus, for simple microcanonical systems,

$$P^o = \frac{1}{n} \qquad (4a)$$

or, if the states are grouped closely enough to define a density of states function $\rho(E)$, of the total energy E, we have,

$$P^{O} = 1/\rho(E) \tag{4b}$$

Using (4) in (1), and further defining the "surprisal"

$$I_i = -\ln\{P_i/P_i^{O}\} \tag{5}$$

we have

$$I = -\sum_i P_i I_i \tag{6}$$

We can see that the information is the negative average value of the surprisal, a quantity which from information theory is the difference of the self-information of the experimental distribution ($-\ln P_i$) and the self-information of the microcanonical distribution ($-\ln P_i^{O}$).

Since P_i represents some combination of statistics and dynamics in an experiment, and P_i^{O} is a purely statistical quantity, the form of the surprisal should then give us relevant dynamical information.

III. SURPRISAL ANALYSIS

To characterize the pumping distributions we now calculate the form of the surprisals. The experimental rates are those of references 6-7 and we use the RRHO approximation to generate simple baseline statistical rates P^{O}. We employ the dimensionless energies f_R, f_V, and f_T which correspond to the fractional product energies in rotation, vibration, and translation, respectively. Thus we must always have

$$f_R + f_V + f_T = 1 \tag{7}$$

The $\{f_x\}$ are calculated according to the total energies with the constraint

$$E_{total} = -\Delta H^{O} + E_a + \tfrac{3}{2}RT + RT \tag{8}$$

where the heat of reaction, $-\Delta H^{O}$, is added to the relative reactant translational energy, $E_a + \frac{3}{2}RT$, plus an additional RT for the internal energy of the incident diatomic.

Rather than working directly with the rotational surprisals, we now compute and analyze the translational surprisals, thereby considering the vibrational and rotational degrees of freedom as components of the internal molecular motion such that

$$f_T = 1 - (f_V + f_R) \equiv 1 - f_{int}. \tag{9}$$

The translational surprisals for different vibrational levels are compared by normalizing P and P^O as though each product vibrational level comprised a separate experiment. Thus, we constrain

$$\sum P(f_T|v) = 1 \tag{10}$$

$$\sum P^O(f_T|v) = 1 \tag{11}$$

where the probabilities are given for each product translational energy, given a vibrational level v. The prior rates are computed according to reference 5:

$$P^O(f_T) = \xi f_T^{1/2}(1-f_T) \tag{12}$$

where ξ is determined to satisfy the normalization by selecting those values of f_T which correspond to experimentally observed J-levels. With this normalization method, we can analyze the deviation from the statistical rate within each v-level without concern for the weighting effects of the vibrational distribution.

The translational surprisals for Reactions (I), (II), (III), (V), (VI), and (VII) are shown in Figures 1-2. It is important to note that the curves are most narrow for the highest observed vibrational levels and broaden for lower levels. In general, the surprisals achieve maximum width in the intermediate vibrational levels. We also note the lack of symmetry in the surprisals. Particularly for Reactions (III) and (VII) the surprisals skew toward the high rotational (low translational) levels, with respect to the most probable J-level, denoted $\hat{J}$. We use $\hat{J}$ for the rotational level at which the surprisal, I, is a minimum. The value of $\hat{J}$ is usually, but not necessarily, equal to that rotational level within a vibrational manifold with the greatest population.

We quantify the full-width of each surprisal by measuring

arbitrarily at I = ln2 , where P = $P^{o}/2$. We see in Table I that for Reactions (I) and (III) the full-widths are greatest in the middle vibrational levels. According to the model described in the next section, the Reaction (II) maximum full width should also occur in a middle vibrational level; we justify this identification later.

IV. A SEMI-EMPIRICAL MODEL TO CORRELATE ROTATIONAL SURPRISAL FUNCTIONS.

As a result of the normalization, all surprisals for a given reaction have roughly equivalent peak magnitudes. The significant variations are in the full-widths of the curves at some arbitrary value of I, and in the degree of skewness. We can directly relate the surprisal widths to the entropy of the distribution. Clearly, as the width shrinks to a single J-level, we have a minimum of entropy (or a maximum of information), i.e., we can make the best possible rotational level prediction for an experiment. As the surprisal broadens ultimately to a horizontal line such that I = 0, we have P = P^{o} and thus a maximum of entropy since the result is simply microcanonical. In a future paper, we quantify the relationship of the surprisal widths to the classical "information" as defined in Eq. 6, and show how the choice of rate normalization is crucial to the use of information as a predictive tool.

We now construct a model to interpret the surprisal results based on reaction complex dynamics as described in references 10-14. Trajectory calculations for three body exothermic reactions of the type A + BC → AB^{+} + C from reference 10 indicate that attractive potential energy surfaces facilitate multiple encounters among the three atoms before separation. A limit is eventually reached where the dissociation of the complex is governed by statistical considerations, as explored by J. C. Light and co-workers in references 15-18. In cases where the potential energy surfaces exhibit a mixture of attractive and repulsive character, we find useful both statistical and dynamical concepts.

The net effect of secondary encounters within the reaction complex is a broadening of the energy and angular distributions, as proposed in references 10-14. The two primary types of encounters are termed "clouting" and "clutching." Clouting involves a repulsive encounter between A and C with consequent reduction in the angular velocity of $AB^{\pm}$. Clutching secondary encounters are also known as "migratory" encounters. The probability of "migration" increases with the magnitude of the attractive part of the potential energy surface, A. Therefore, for example, we would expect migration to play a greater role in Reactions (III) and (VII) where A ≈45% than in Reaction (V) where A ≈25% (references 7 and 19).

A further effect cited in references 10-14 is an observed decrease in the mean product vibrational energy, $\langle E_{vib} \rangle$, with increasing collision complexity resulting from increasing A. The result is conversion of vibrational energy to rotation and translation. Product rotational energy is particularly enhanced for migratory encounters.

Dramatic migratory effects for the reactions H + ICl → HCl + I, H + ClBr → (HCl + Br, HBr + Cl) resulting in bimodal rotational distributions within each product vibrational level are described in reference 13. Applying these concepts to Reactions (I)-(VIII), we anticipate, and in fact, observe both broadened and skewed rotational distributions with the most attractive potential energy surfaces exhibiting the largest asymmetry toward high rotational levels.

A model which combines these dynamical ideas with statistics must predict the vibrational dependence of both the surprisal full-widths and the degree of asymmetry or skewness. A schematic of the model is shown in Figure 3. For pedogogical purposes Reaction (I) is used since only three v-levels are involved.

As the reaction begins, a particular product vibrational energy becomes most probable depending on a given trajectory through the potential energy surface. This vibrational energy may be quickly transformed into rotational and translational energy via clouting or clutching secondary encounters followed by repulsive energy release.

In order to model these interactions we assume that the energy redistribution in vibration, rotation, and translation (V, R, and T) can be described by a redistribution of V and R states within the fully formed molecule--HF for example in Reactions (I) and (III). Use of the product V and R states is especially reasonable in Reactions (II)-(VIII) in which the "light-atom anomaly" results in an "AB" bond being effectively formed before the "C" atom becomes involved. This allows use of the unperturbed product states as an approximation to the time-dependent reaction complex wave functions.

For the specific case shown in Figure 3 we see that the v=1 population will result partly from molecules initially choosing the v=1 product level and partly from molecules choosing levels v=2 and v=3 and undergoing the energy redistribution process. The redistribution path is taken to be from vibration resonantly to rotation and then in part to translation. This would seem to follow the order taken in the complex. A direct path from vibration to a mixture of rotation and translation was also tested with significantly inferior results.

The contributions from the higher V-levels must be weighted according to the initial transition state vibrational probability, $P(E_{V-R})$, and the amount of rotational energy, ΔE, converted into product translational energy. The term E_{V-R} denotes the energy resonance among the selected V-R states. If the initial populations are taken as grouped within equally small energy intervals, Δ', the redistribution process makes these states available to lower V-levels. The natural logarithm of the number of weighted available states then corresponds to the entropy, or width, of the given distribution.

We take $P(E_{V-R})$ equal to the final vibrational population, P(v). We find that although the model predicts a large difference between the <u>absolute</u> reaction complex and final vibrational populations, the <u>relative</u> (normalized) populations are almost unchanged. We see in fact a small relative population shift to lower v-levels, but the differences are actually within the experimental uncertainties of the vibrational

distribution. Each state is also weighted by a factor $e^{-E/kT}$ which gives the probability for relaxation from a selected state to the most probable rotational state, J, an energy distance ΔE away. The adjustable parameter "α" is a measure of the magnitude of the energy redistribution process for a given reaction. It is analogous to the reciprocal of the constant "C_2" as given by Polanyi and Woodall in reference 20 for HF collisional rotational relaxation:

$$P_{J}^{J'} = C_1 \exp(-C_2 \Delta E/kT) \qquad (13)$$

where $\Delta E = E_{J'} - E_J^0$. Each rotational level found within the interval ΔE before the final rotation to translation redistribution is weighted by its degeneracy, 2J+1.

Performing the sum

$$N'(v) = \sum_{\substack{\text{selected} \\ J \text{ levels}}} (2J+1) P_{J_{J-E}} e^{-E/kT} \qquad (14)$$

gives us an adjusted number of states which contributes to the rotational surprisal width or entropy of the distribution. Identifying the surprisal width with the logarithm of the number of weighted available states gives

$$\text{width}(v) = S(v) = C \ln N'(v) \qquad (15)$$

where C is a constant independent of v.

V. APPLICATION OF THE MODEL

The predictions from equation (15) for reactions (III), (V), (VI), and (VII) are compared with experimental widths in Figure 4 for optimum values of α. The value of C is fixed by matching the largest width with the largest value of $\ln N'$. We find in fact a smooth functional relationship between α and C such that for a given energy interval, as α increases, C decreases. For large values of α ($\alpha > 9$), $dC/d\alpha$ is small and negative, implying a nearly constant value for C for several values of α. This well-defined correspondence between α and C will be used in predicting distributions for reactions (IV) and (VIII).

We select an energy interval, Δ' (see Figure 3), approximately equal to twice the smallest surprisal width and then vary the parameter α. (In practice the specific choice of interval has little effect on the results as long as it is reasonably small.) For small α, we find that high J-levels are not contributing enough to the rotational width, while at large α the contribution is too great. The optimum value of α is determined by locating the minimum in the standard deviation function $\sigma = \sigma(\alpha)$ where:

$$\sigma^2 = \frac{1}{N} \sum_{v=1}^{N} [I(v,\alpha)_{\text{predicted}} - I(v,\alpha)_{\text{observed}}]^2 \qquad (16)$$

In Reaction (III) for example, using data for the first five vibrational levels results in a pronounced minimum for $\sigma(\alpha)$ at $\alpha = 14$. For Reaction (I), although there are widths to correlate at only $v = 1$ and $v = 2$, we find an optimum $\alpha = 6$. Here we used the $v = 3$ surprisal width as half the energy interval.

The Reaction (II) rotational distribution for v=2 was determined by Polanyi (reference 6) with considerably less accuracy than for the $v = 3$ and $v = 4$ levels. Furthermore, the $v = 1$ distribution was estimated since he observed no detectable emission in that band. If we apply our techniques to Reaction (II), assuming $\alpha = 6$, we can then generate a rotational distribution for the first vibrational level as shown in Fig. 5. The data was generated using parameters from the other vibrational levels. This results in large entropy rotational distributions in the middle v-levels for Reaction (II) as we have already observed for Reactions (I) and (III). We show the results for Reactions (I) and (II) in Table II.

The parameter "α" is taken physically as the strength of interaction for the secondary encounters in the model. Large values of α denote higher probabilities for redistribution over significant values of ΔE. We assume that α is dependent on the potential energy surfaces and the macroscopic reaction initial conditions. Thus α may well be approximately isotopically independent, particularly between Reactions (III) and (IV)

and between (VII) and (VIII). We note that the optimum values of both α and ζ for Reactions (V) and (VI) are very close, indicating that isotopic independence of these parameters is a reasonable assumption. Using this assumption we can generate the surprisal widths predicted by the model for reactions (IV) and (VIII) as shown in Figure 6. It is not surprising that the widths for Reactions (IV) and (VIII) generally exceed those of Reactions (III) and (VII) since the deuterium product energy levels are closer together, facilitating energy level mixing.

As an almost independent check on the model, we now predict the degree of asymmetry for rotational surprisals in reactions characterized by attractive surfaces. We expect rotational asymmetry in migratory encounters which may enhance product rotation as opposed to repulsive, glancing encounters which tend to restrict product rotational energy. If we now compare the probability of energy transfer to a low J-level (at say $I = \ln 2$) with that of a high J-level (also at $I = \ln 2$) we obtain a quantitative measure of the asymmetry, i.e., a comparison of the "half-widths" of the distributions centered about each $\hat{J}$.

Therefore consider an intermediate state with energy E_o which transforms within a v-level either to a low J-level of energy E_1, or to a high J-level of energy E_2. The ratio of these two probabilities according to a collisional relaxation analogy is then

$$\frac{P(E_o \rightarrow E_1)}{P(E_o \rightarrow E_2)} = \frac{e^{-(E_o-E_1)/\alpha kT}}{e^{-(E_o-E_2)/\alpha kT}} = e^{-(E_2-E_1)/\alpha kT} \tag{17}$$

If $E_2 - E_1$ is given as the energy width of a translational surprisal, then we can predict the ratio of "half-widths" as

$$\frac{\Delta_1}{\Delta_2} = e^{-(E_2-E_1)/\alpha kT} \tag{18}$$

where:

$$\Delta_1 = f_T(I = \ln 2 \text{ at low } J) - f_T(\hat{J}) \tag{19a}$$

$$\Delta_2 = f_T(\hat{J}) - f_T(I = \ln 2 \text{ at high } J) \tag{19b}$$

$$E_1 = f_T(I = \ln 2 \text{ at low } J) \tag{19c}$$

$$E_2 = f_T(I = \ln 2 \text{ at high } J) \tag{19d}$$

$$\Delta_1 + \Delta_2 \equiv \Delta = E_2 - E_1 \tag{19e}$$

A comparison of Equation 18 with the actual half-widths for Reaction (III) is shown in Figure 7. We see that for the same values of Δ we obtain good predictions for both the half-widths and the full-widths. The same technique was applied to Reaction (VII) with less quantitative success due primarily to the simplicity behind equations (17)-(19) in estimating redistribution probabilities. The model does exhibit qualitative success in predicting Reaction (VII) asymmetry and could be made more sophisticated except that our intent is to provide a simple model for correlating product distributions.

We now develop a simple algorithm to regenerate the rate coefficients for Reaction (III) based on the model. Using the translational surprisals we note that most of the curves can be approximated by a linear function for $f_T < f_T(\hat{J})$ and a quadratic function for $f_T > f_T(\hat{J})$. So for large f_T, we find "A" such that

$$I - I(J) = A[f_T(I = \ln 2) - f_T(\hat{J})]^2 \tag{20}$$

where $I = \ln 2$ and $f_T(\hat{J})$ is the value of f_T at the maximum value (peak) of $[-I(f_T)]$. The term $f_T(I = \ln 2)$ is determined by knowing that

$$\Delta_1 + \Delta_2 = \Delta = C\ln\Omega' \tag{21}$$

and

$$\Delta_1/\Delta_2 = e^{-\Delta/kT} \tag{22}$$

Combining Equations 21 and 22 gives

$$\Delta_1 = \frac{\Delta}{1+e^{-\Delta/kT}} \tag{23}$$

and

$$\Delta_2 = \frac{\Delta}{1+e^{+\Delta/kT}} \tag{24}$$

Then for large f_T (small f_R) we have

$$f_T(I = \ln 2 \text{ at low } J) = f_T(\hat{J}) + \Delta_1 \tag{25}$$

$\hat{I}(\hat{J})$ is determined by observing that each product rotational distribution has total population roughly proportional to the width times the height of the distribution. Thus, we set

$$P(\hat{J}) = \frac{\gamma P(v)}{\bar{\ }} \tag{26}$$

where γ is fixed to make the largest value of $P(\hat{J})$ for the entire vibrotational distribution equal to unity. Now inverting Equation 5 and combining with Equation 12 we have for any value of f_T:

$$P(f_T) = \kappa(v) P^{\circ}(f_T) e^{-I(f_T)} \tag{27}$$

where

$$\kappa(v) = \sum_{\bar{J}} P'(J|v) \tag{28}$$

with P' as the experimental distribution observed in reference 7. The last two formulas are simply the inversion of the normalization method employed previously. For $I(\hat{J})$ we now have:

$$I(\hat{J}) = -\ln\left(\frac{P(\hat{J})}{\kappa P^{\circ}(J)}\right) = -\ln\left(\frac{\gamma P(v)}{\kappa P^{\circ}}\right) \tag{29}$$

For $f_T < f_T(\hat{J})$ we find the equation of a line through the points $[f_T(\hat{J}),\ I(\hat{J})]$ and $[f_T(\hat{J})-\Delta_2,\ I = \ln 2]$. Using the linear and quadratic forms for the surprisals as functions of f_T, we can now generate the actual distribution $P = P(f_T)$ by using Equation 27 for each selected value of f_T.

Figure 8 compares with our semi-empirical model prediction for the Reaction (III) rate coefficients with the experimental data in terms of f_R. The model also gives qualitative agreement with the Reaction (VII) experimental data although the simplicity of the algorithm results in some quantitative differences.

VI. RATE COEFFICIENT PREDICTION FOR REACTIONS (IV) and (VIII)

We now apply the model with some additional assumptions to Reactions (IV) and (VIII) for which, to the best of our knowledge, detailed experimental rate coefficients are not yet available. To develop the full vibrotational distribution we must predict a vibrational pumping distribution, a most probable $\hat{J}$ within

each v-level, and the form of the rotational surprisals for each v-level. Berry has reported in reference 21 an isotopic independence for the vibrational surprisals of Reactions (I) and (II). The linearity of these surprisals indicates that the distribution is characterized by just one moment, namely the mean product vibrational energy. The vibrational surprisals for Reactions (III) and (VII) are computed using the RRHO result

$$P^{O}(f_v) = 8\ (1-f_v)^{3/2} \tag{30}$$

such that

$$\sum_v P^{O}(f_v) = 1 \tag{31}$$

The resultant surprisals are not entirely linear, but are regular enough so that if we assume an isotopic independence we can predict $I(f_v)$ for the product DF and DBr molecular vibrational levels. Then using the predicted values I(v) we find the vibrational distribution

$$P(v) = \kappa_v\ P^{O}\ e^{-I} \tag{32}$$

where κ_v is such that the largest value of P(v) is unity. This normalization giving $P(v)_{max} = 1$ is the same used by Polanyi in reference 7.

There is also reported (see reference 22) an isotopic independence for $\hat{f}_R$ as a function of f_v between Reactions (I) and (II). Assuming the same relationship between Reactions (III) and (IV) and between (VII) and (VIII) we can predict $\hat{J}(v)$ for Reactions (IV) and (VIII).

To predict the rotational surprisals according to the model, we use the widths predicted in Figure 6, and the same prescription as given in Section V for Reaction (III). We further identify that only one rotational level beyond the full-width is selected. The full vibrotational distributions for Reactions (IV) and (VIII) thereby generated are shown in Figures 9 and 10.

VII. SUMMARY

A model was developed which combines statistical ideas with well-established reaction dynamics. The model describes the features of experimental rotational distributions for six reactions and predicts the full vibrotational distributions for two reactions not yet determined experimentally. Future work involves defining the relationships among arbitrary rotational distributions and the classical "information" of a distribution for a given reaction. We also hope to extend the ideas presented here to collisional relaxation processes.

TABLE I. Translational Surprisal Full-Widths, $\Delta(f_T)$, at I=.n 2

Reaction (I)

V	Δ
1	0.198
2	0.212
3	0.045

Reaction (II)

V	Δ
1	0.181
2	0.147
3	0.122
4	0.054

Reaction (III)

V	Δ
1	0.036
2	0.048
3	0.065
4	0.068
5	0.064
6	0.068
7	0.030
8	0.017

TABLE II. Translational Surprisal Full-Widths, $\Lambda(f_T)$, at I=in 2.

Reaction (I)

V	Λ observed	Λ predicted (n=6)
1	0.198	0.208
2	0.212	0.212

Reaction (II)

V	Λ observed	Λ predicted (n=6)
1	0.181	0.117
2	0.147	0.147
3	0.122	0.131

The model predictions are compared with the observed data for Reactions (I) and (II). Note that the precise match for the largest full-widths is simply due to the normalization of equation (15).

References

1. N. Cohen and J. F. Bott, SAMSO Report TR-76-82, 15 April 1976.

2. N. Cohen, SAMSO Report TR-78-41, 8 June 1978.

3. R. B. Bernstein and R. D. Levine, J. Chem. Phys. 57, 434 (1972)

4. A. Ben-Shaul, R. D. Levine, and R. B. Bernstein, J. Chem. Phys. 57, 5427 (1972).

5. R. B. Bernstein and R. D. Levine, Adv. in At. and Mol. Phys. 11, 215 (1975).

6. J. C. Polanyi and K. B. Woodall, J. Chem. Phys. 57, 1574 (1972).

7. J. C. Polanyi and J. J. Sloan, J. Chem. Phys. 57, 4988 (1972).

8. K. G. Anlauf, D. S. Horne, R. G. MacDonald, J. C. Polanyi, and K. B. Woodall, J. Chem. Phys. 57, 1561 (1972).

9. P. Pechukas, Dynamics of Molecular Collision--Part B, 269 (1976).

10. P. J. Kuntz, E. M. Nemeth, J. C. Polanyi, S. D. Rosner, and C. E. Young, J. Chem. Phys. 44, 1168 (1966).

11. P. J. Kuntz, E. M. Nemeth, and J. C. Polanyi, J. Chem. Phys. 50, 4607 (1969).

12. P. J. Kuntz, M. H. Mok, and J. C. Polanyi, J. Chem. Phys. 50, 4623 (1969).

13. J. C. Polanyi and W. J. Skrlac, Chemical Physics 23, 167 (1977).

14. J. C. Polanyi and J. L. Schreiber, Physical Chemistry--Vol. VI4, 383 (1974).

15. J. C. Light, J. Chem. Phys. 40, 3221 (1964).

16. P. Pechukas and J. C. Light, J. Chem. Phys. 42, 3281 (1965).

17. P. Pechukas, J. C. Light, and C. Rankin, J. Chem. Phys. 44, 794 (1966).

18. J. C. Light and J. Lin, J. Chem. Phys. 43, 3209 (1965).

19. K. G. Anlauf, P. J. Kuntz, D. H. Maylotte, P. D. Pacey, and J. C. Polanyi, Discuss. Faraday Soc. 44, 183 (1967).

20. J. C. Polanyi and K. B. Woodall, J. Chem. Phys. 56, 1563 (1972).

21. M. J. Berry, J. Chem. Phys. 59, 6229 (1973).

22. R. D. Levine, B. R. Johnson, and R. B. Bernstein, Chem. Phys. Ltrs. 19, 1 (1973).

LIST OF FIGURES

Reactions (III) and (IV) and between (VII) and (VIII).

Figure 7. The ratio of predicted surprisal "half-widths" (Δ) compared with observed data (O) for Reaction (III). Data for Reaction (VII) shows qualitative agreement, although quantitative discrepancies arise due to the simplicity of characterizing the rotational energy distance, δE, as the difference of each selected level energy and $\hat{f}_R$. Constructing a model using a continuum value for δE as the difference between each selected level energy and weighted values of the product rotational distribution energies might improve quantitative results, but would also involve unwarranted complexity in an otherwise simple model.

Figure 8. Predicted (Δ) and experimental (O) product rotational distributions for Reaction (III). Note that the results are best in v-levels where the model accurately predicts the surprisal full-widths. Reaction (VII) data exhibits qualitative agreement although quantitative discrepancies arise due to the simplicity of the model techniques, as alluded to in the caption to Figure 7.

Figure 9. Predicted product distributions for Reaction (IV).

Figure 10. Predicted product distributions for Reaction (VIII).

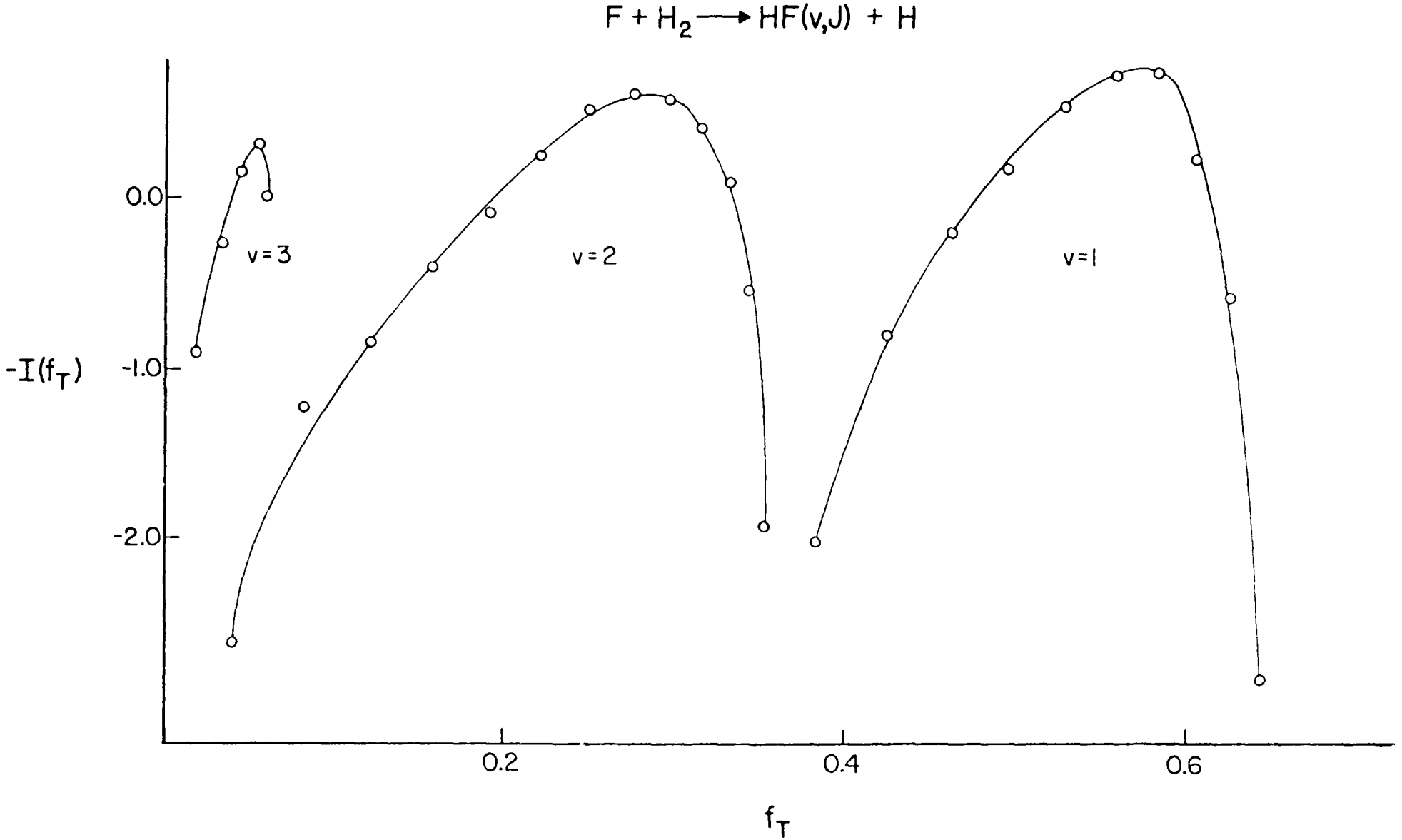

Figure 1a.

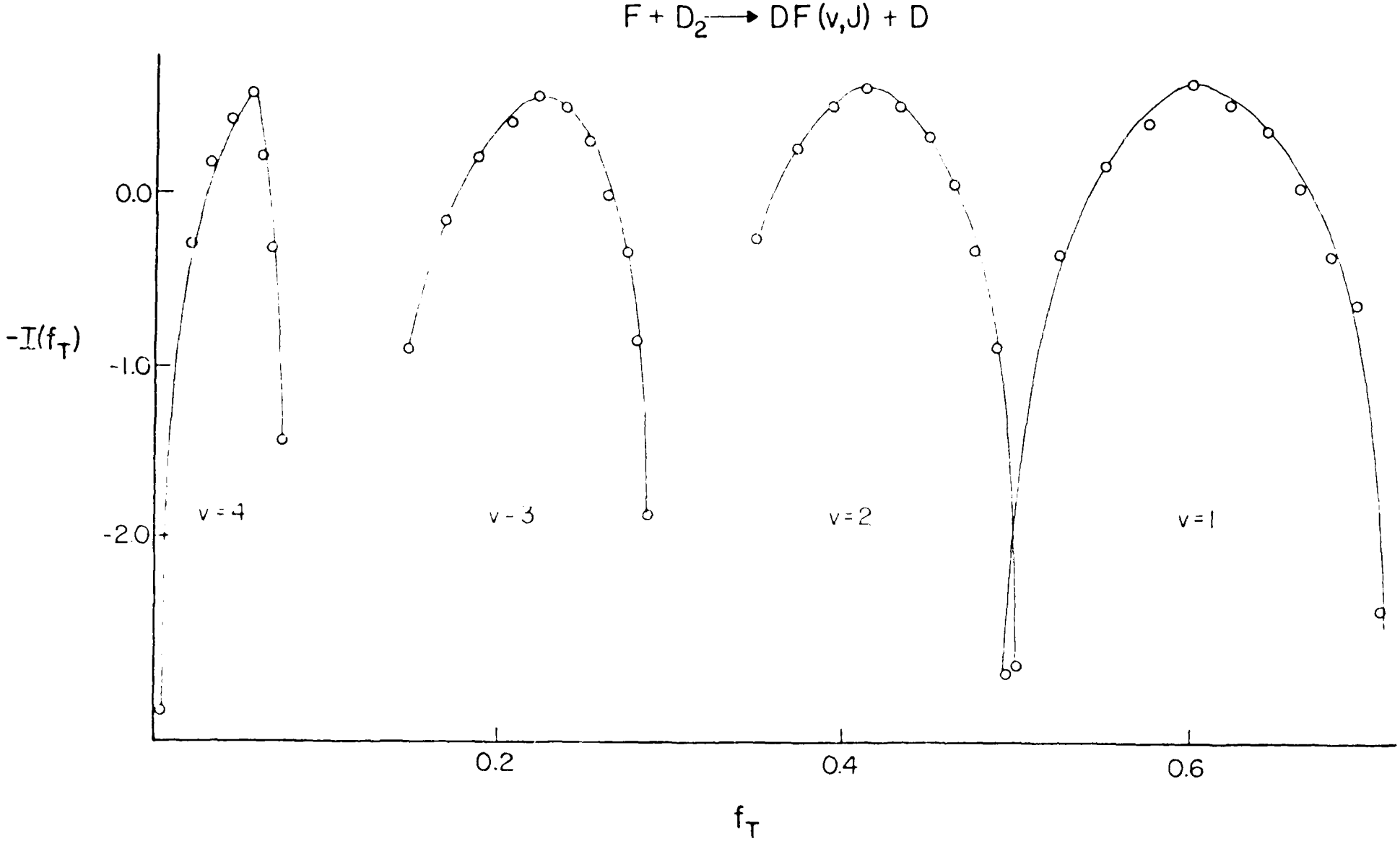

Figure 11b.

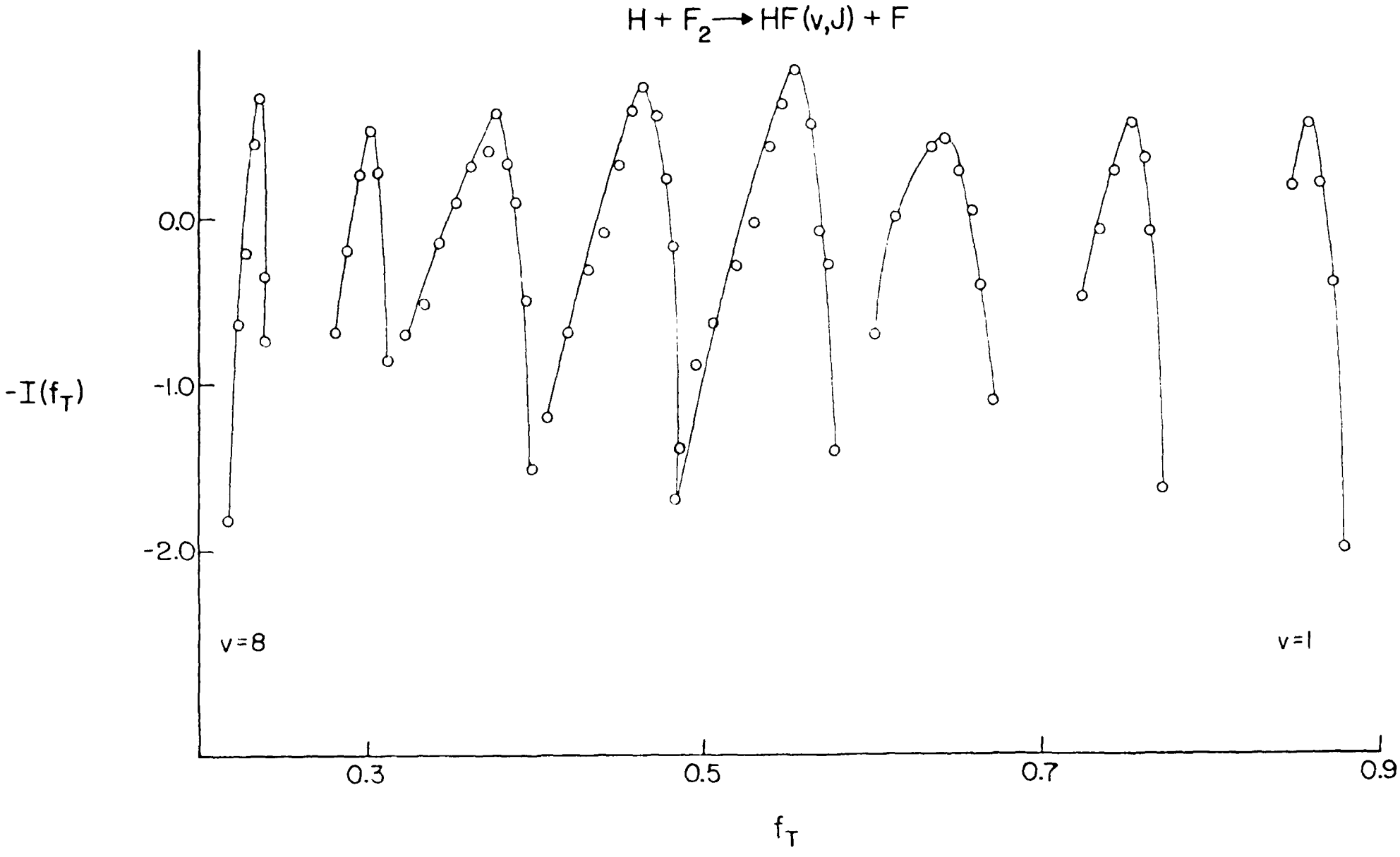
H + F2 → HF(v,J) + F
0.0
-1.0
-2.0
-I(fT)
v=8
v=1
0.3
0.5
0.7
0.9
fT

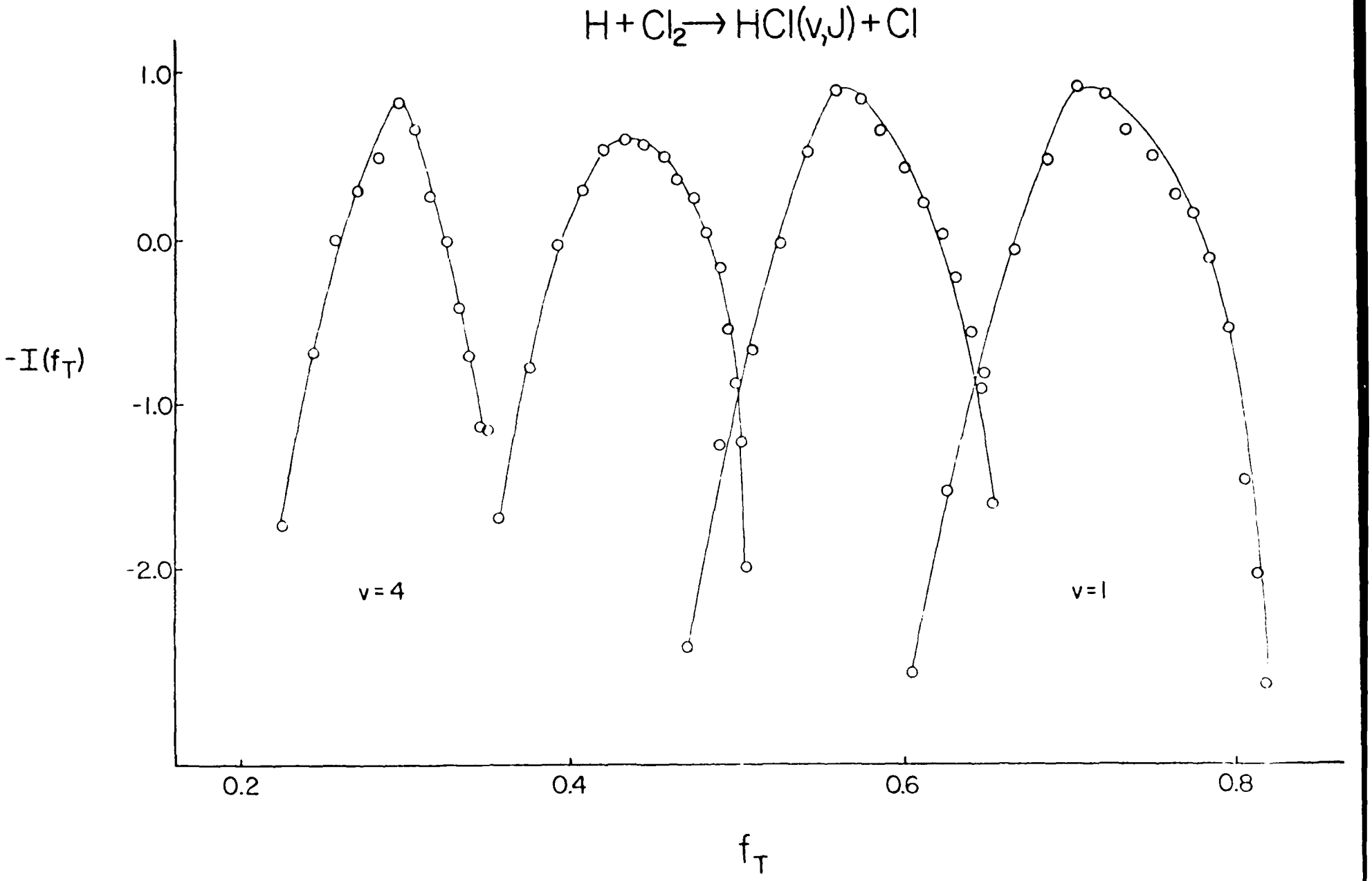

Figure 2a.

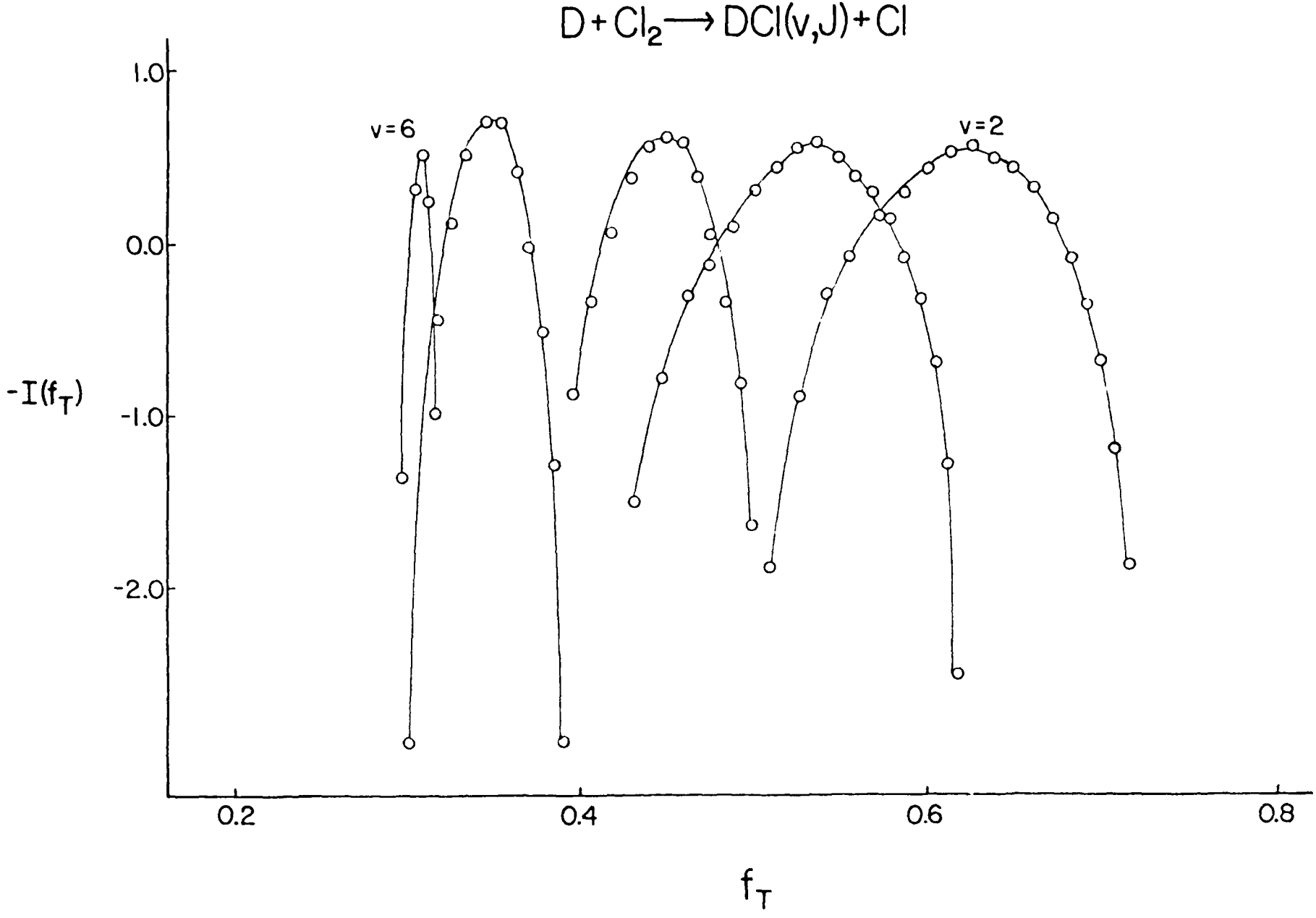

Figure 2b.

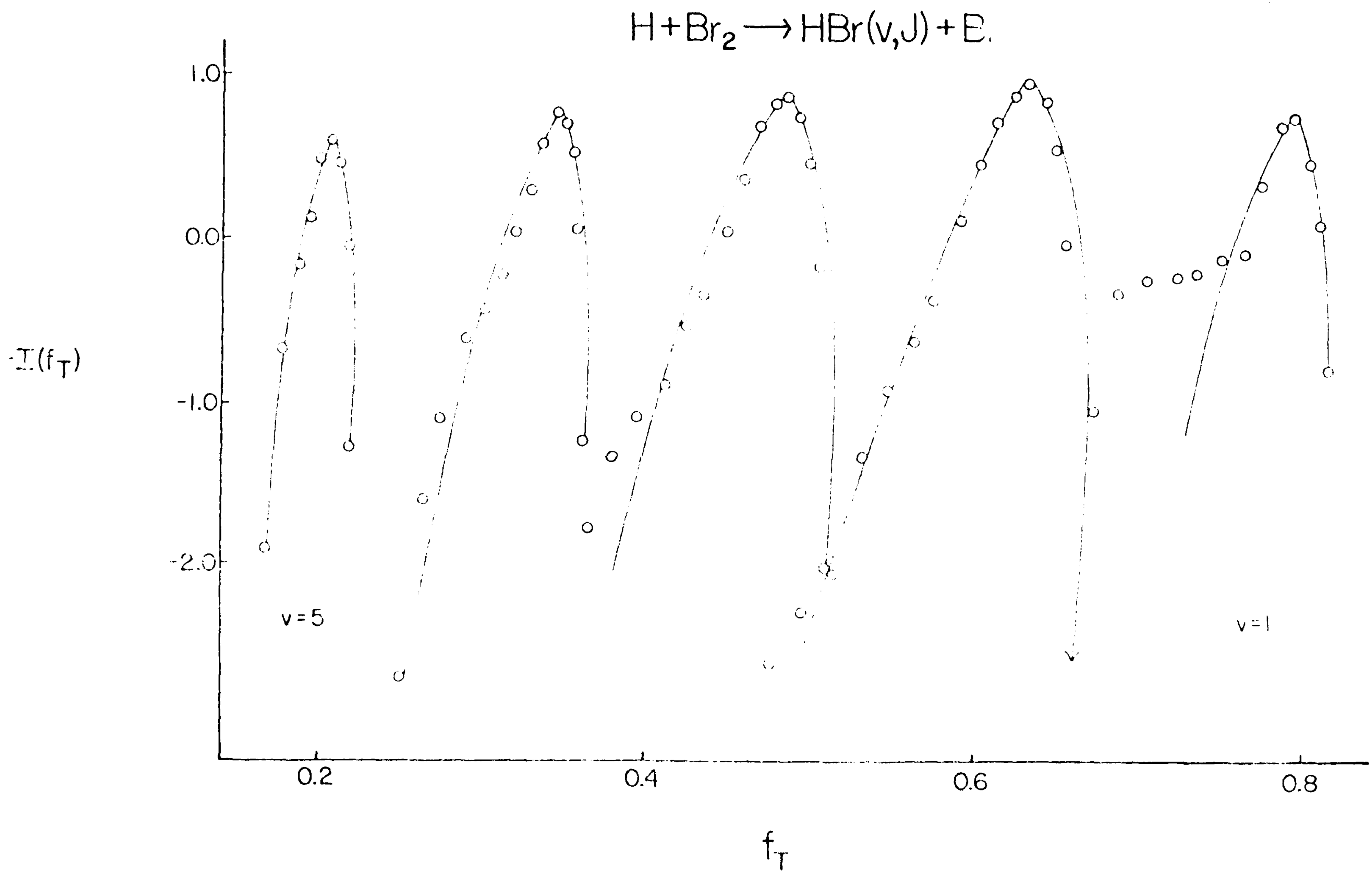

Figure [illegible].

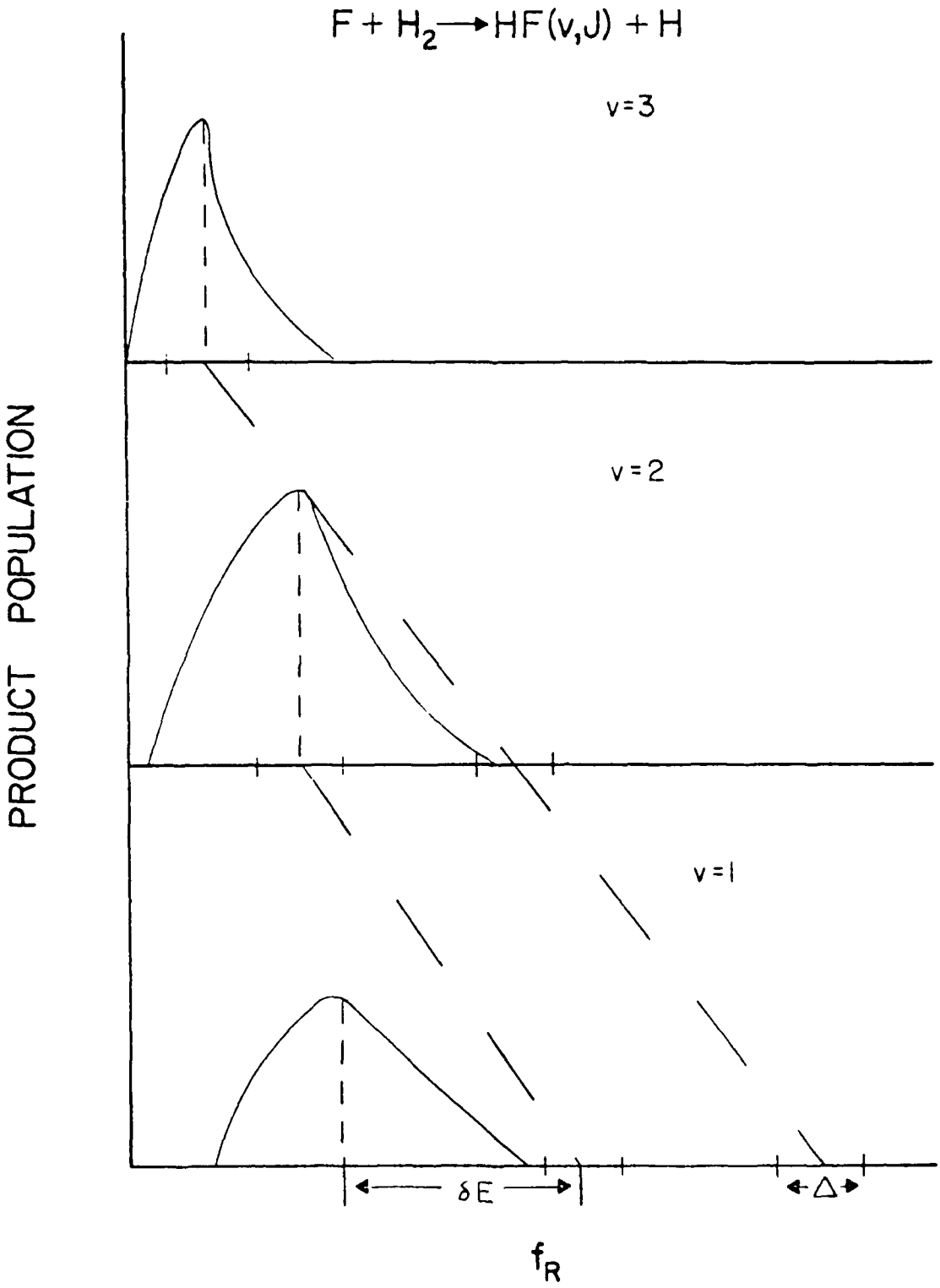

Figure 3.

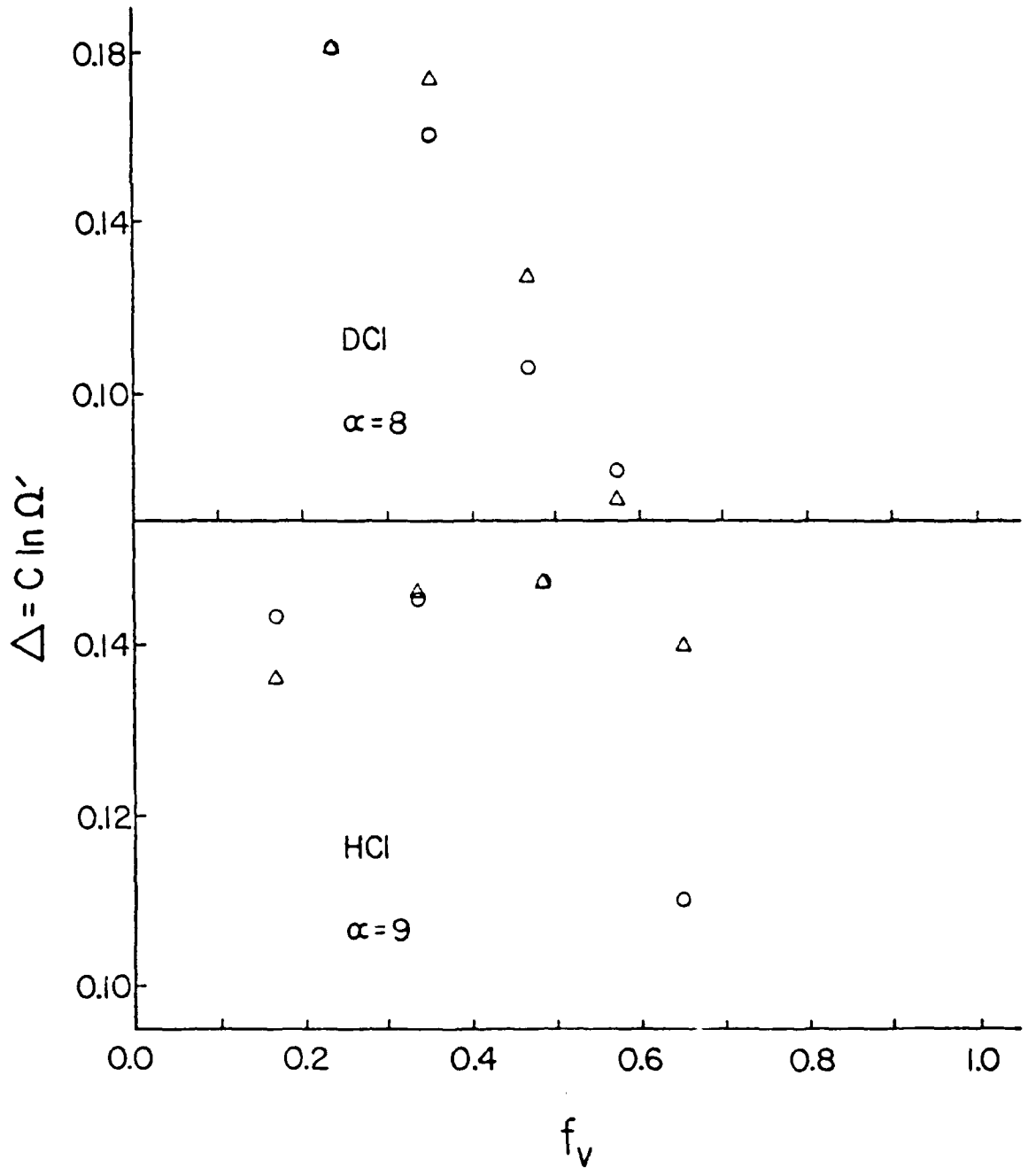

Figure 4a.

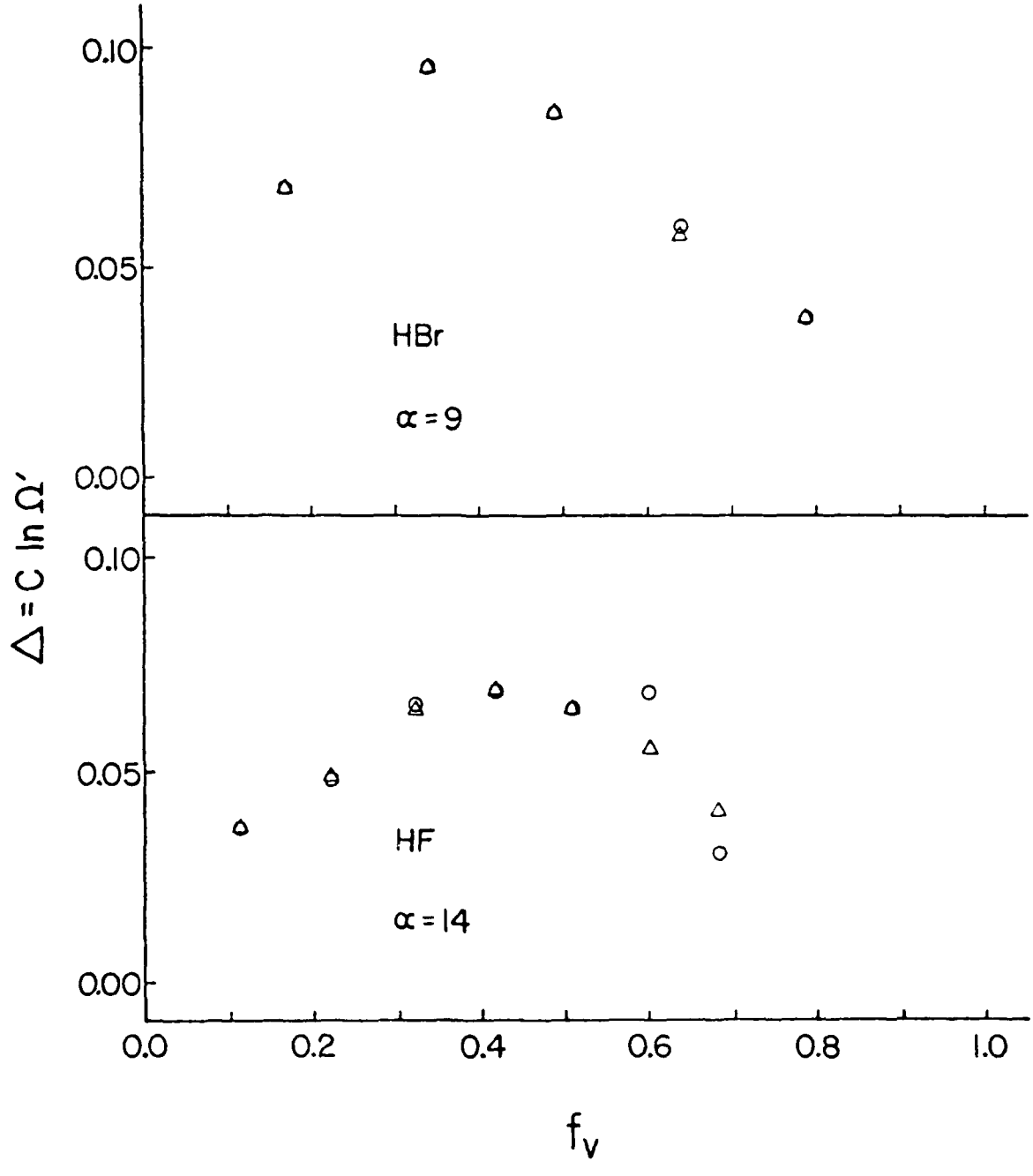

Figure 4b.

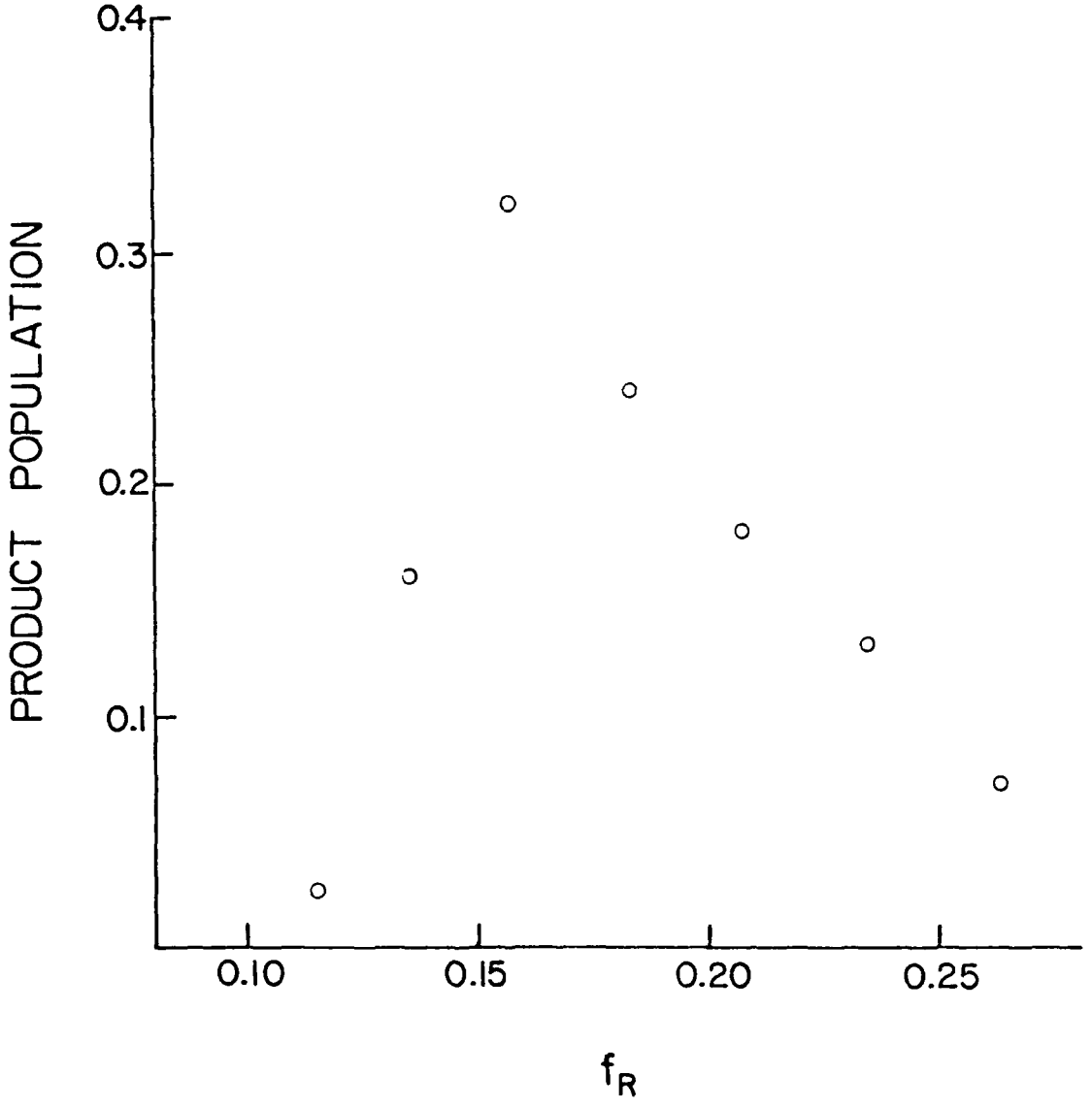

Figure 5.

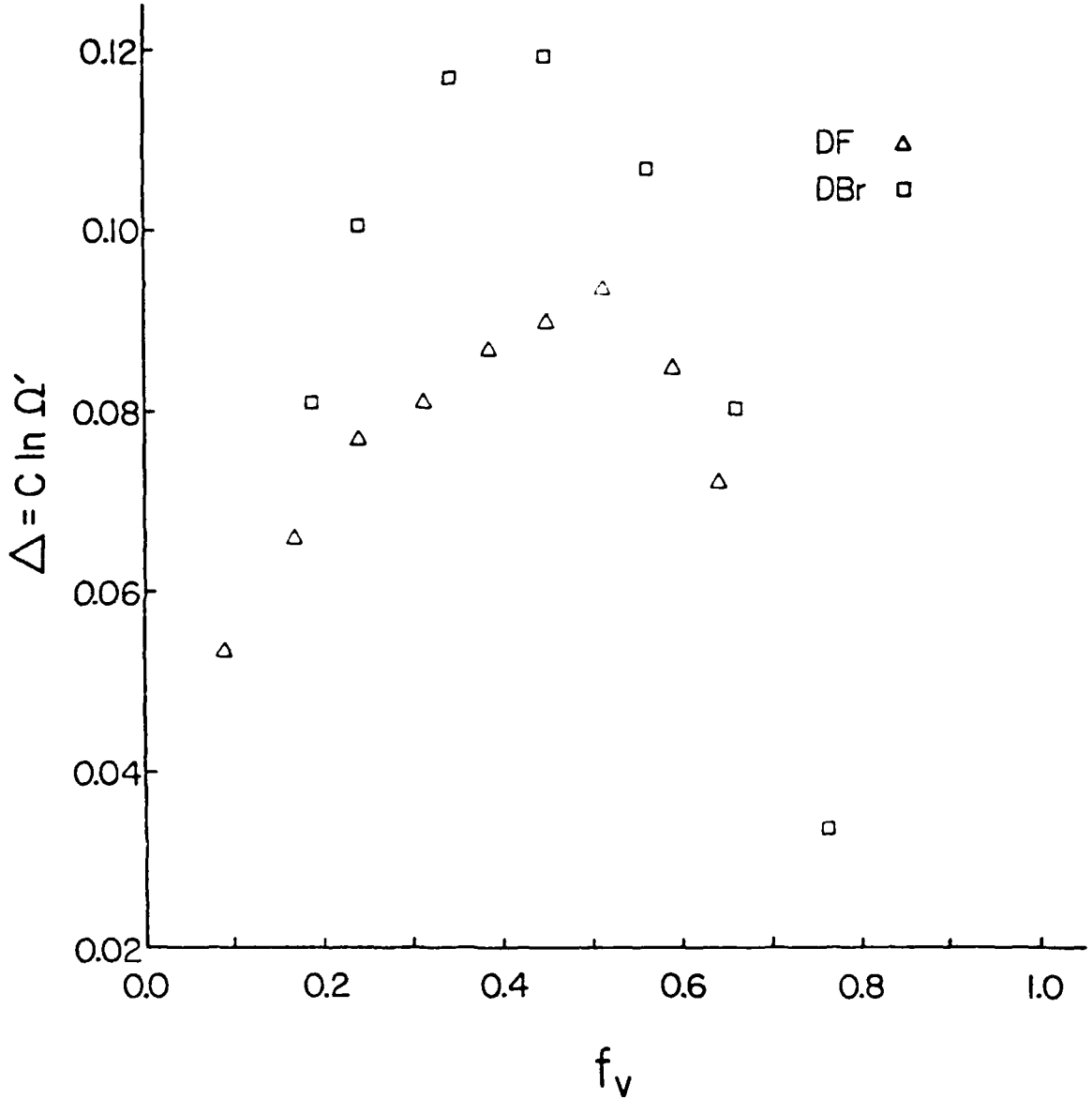

Figure 6.

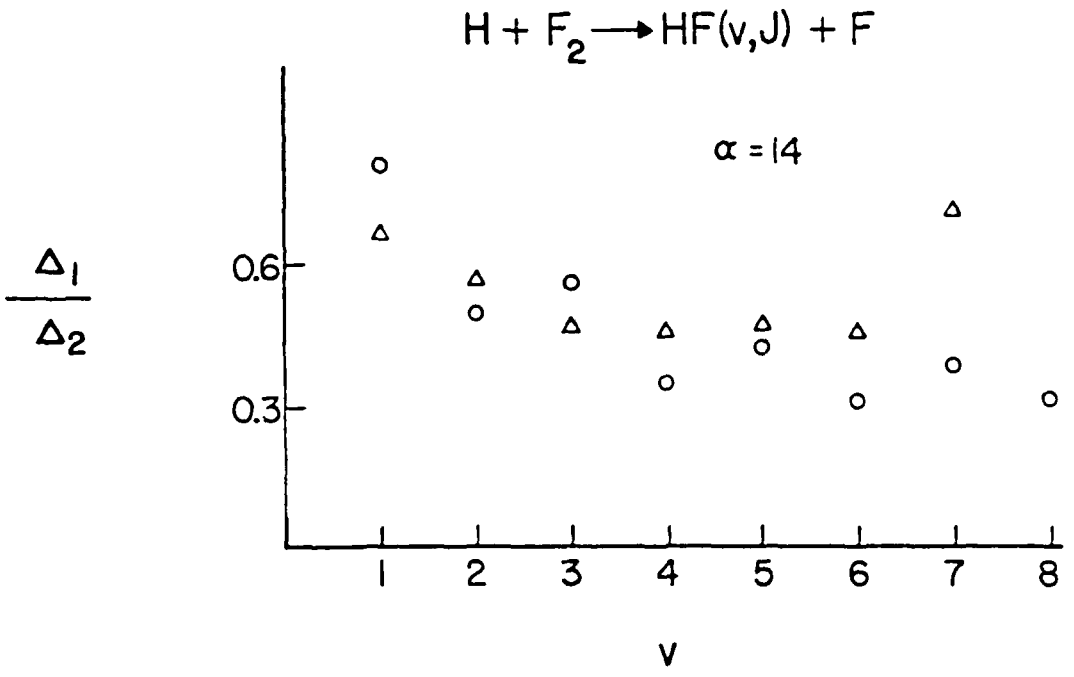

Figure 7.

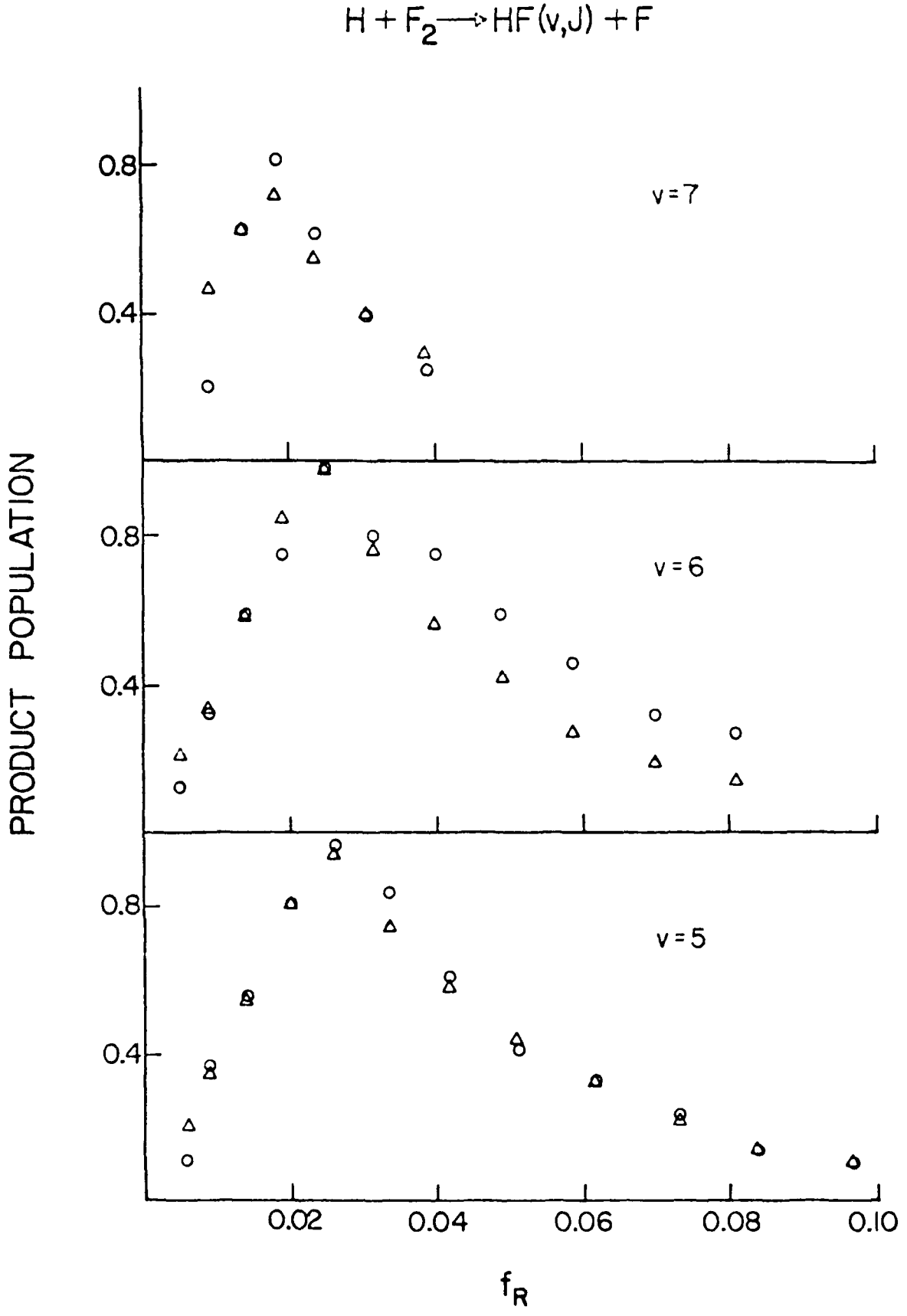
H + F2 ⟶ HF(v,J) + F
PRODUCT POPULATION
0.8
0.4
v=7
0.8
0.4
v=6
0.8
0.4
v=5
0.02
0.04
0.06
0.08
0.10
fR

Figure 8a.

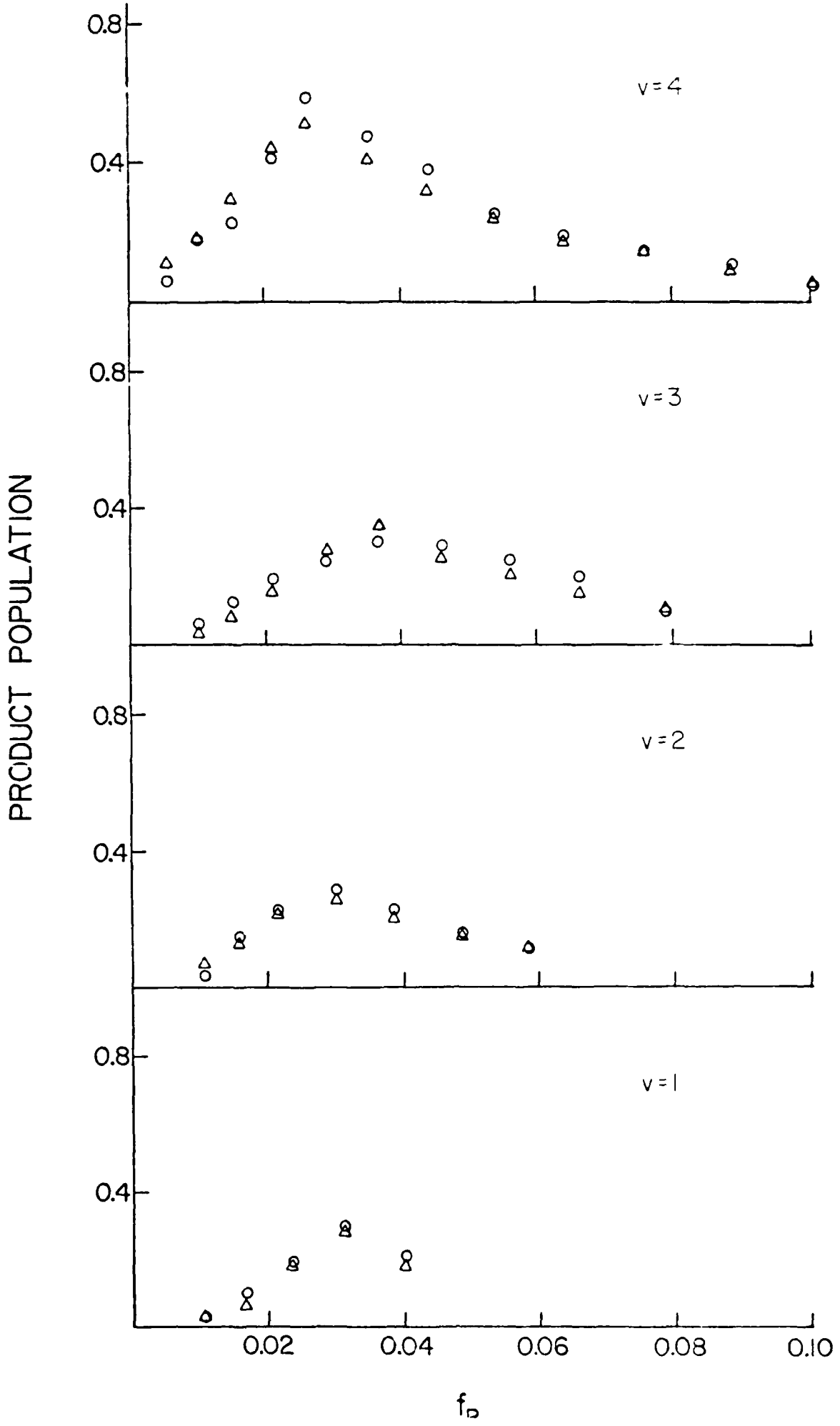
PRODUCT POPULATION
0.8
0.4
v=4
v=3
v=2
v=1
0.02
0.04
0.06
0.08
0.10
f_D

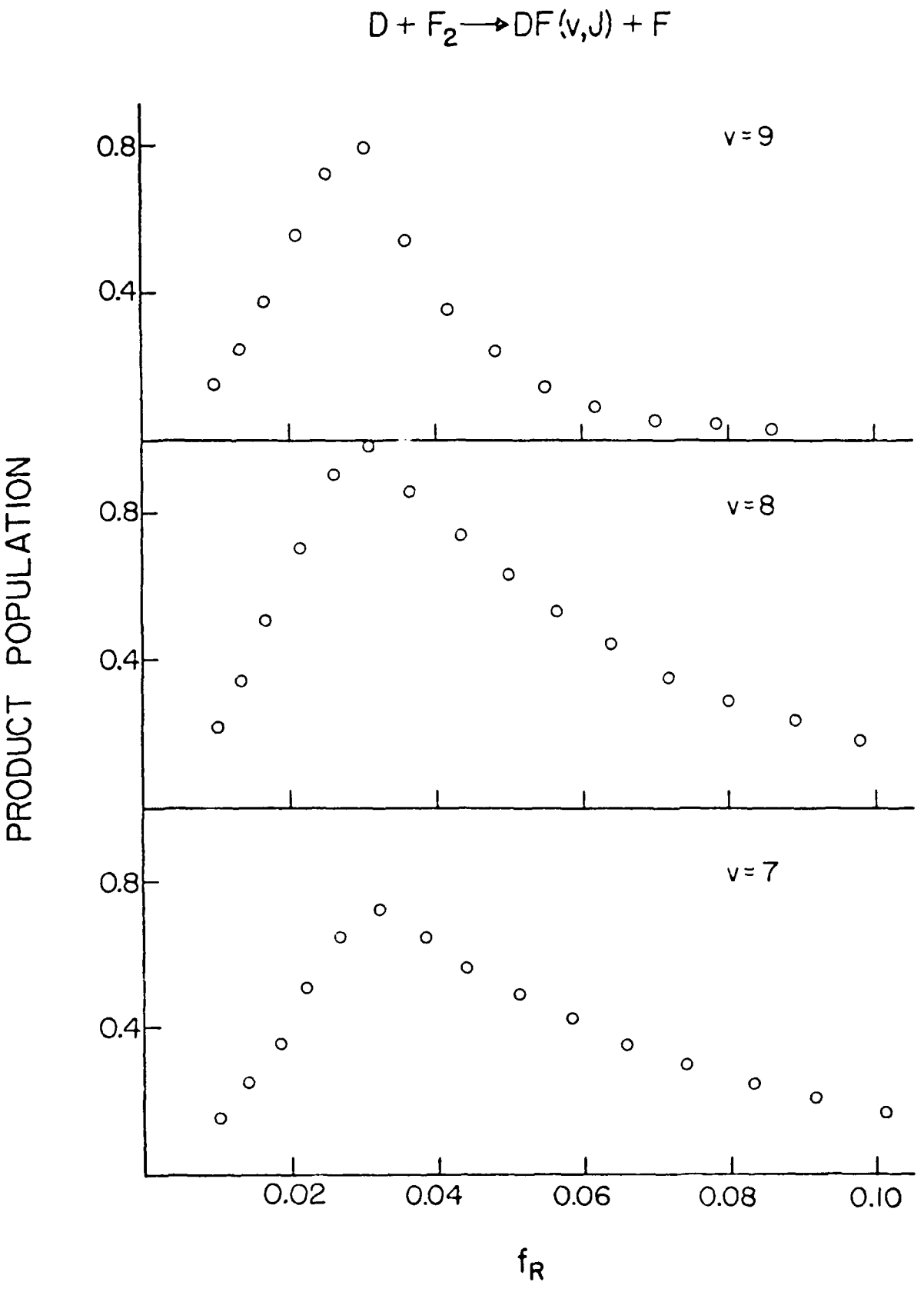
D + F2 → DF(v,J) + F
v = 9
v = 8
v = 7
0.8
0.4
PRODUCT POPULATION
0.02
0.04
0.06
0.08
0.10
fR

Figure 9a.

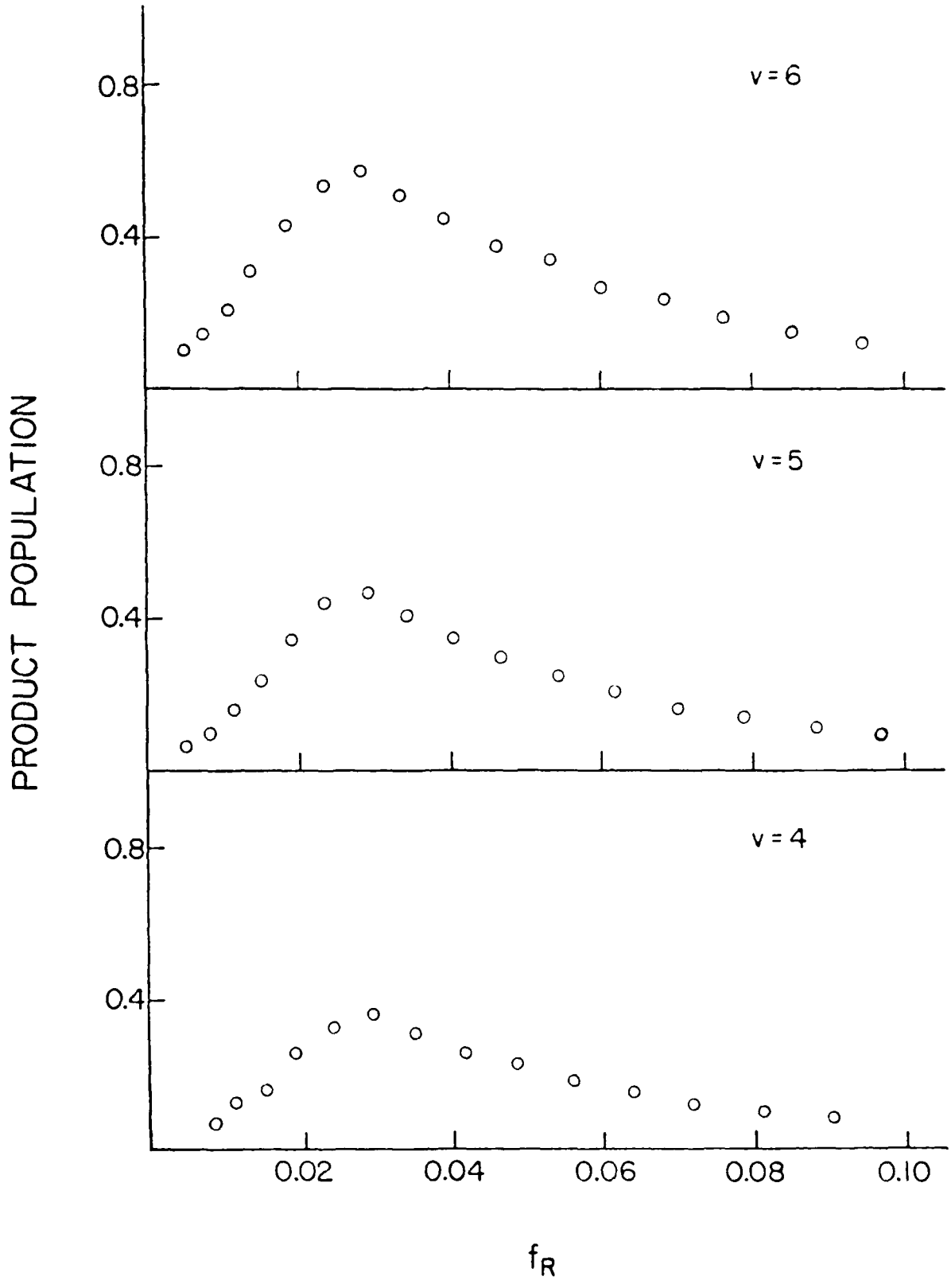
PRODUCT POPULATION
0.8
0.4
v = 6
0.8
0.4
v = 5
0.8
0.4
v = 4
0.02
0.04
0.06
0.08
0.10
f_R

Figure 9b.

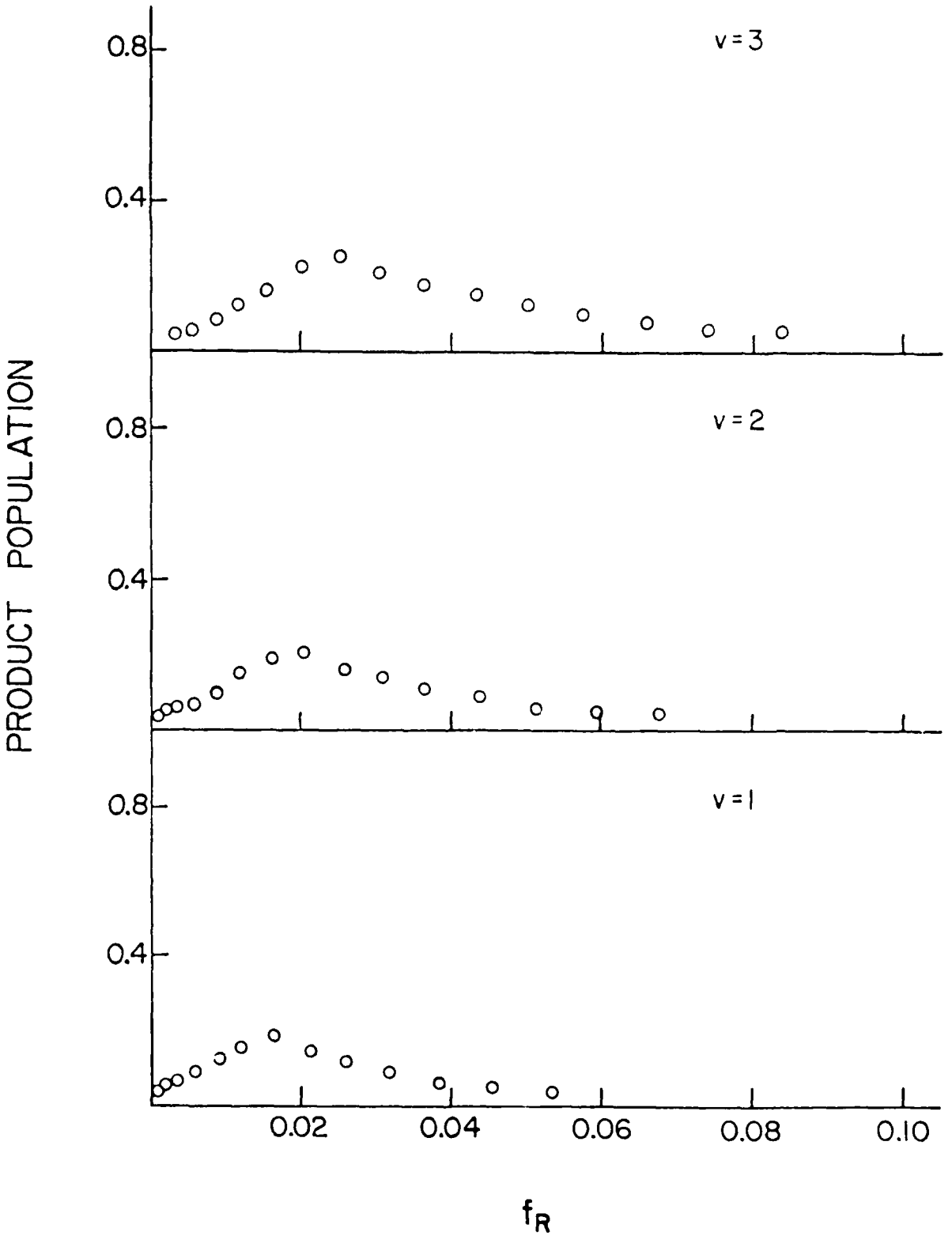

Figure 9c.

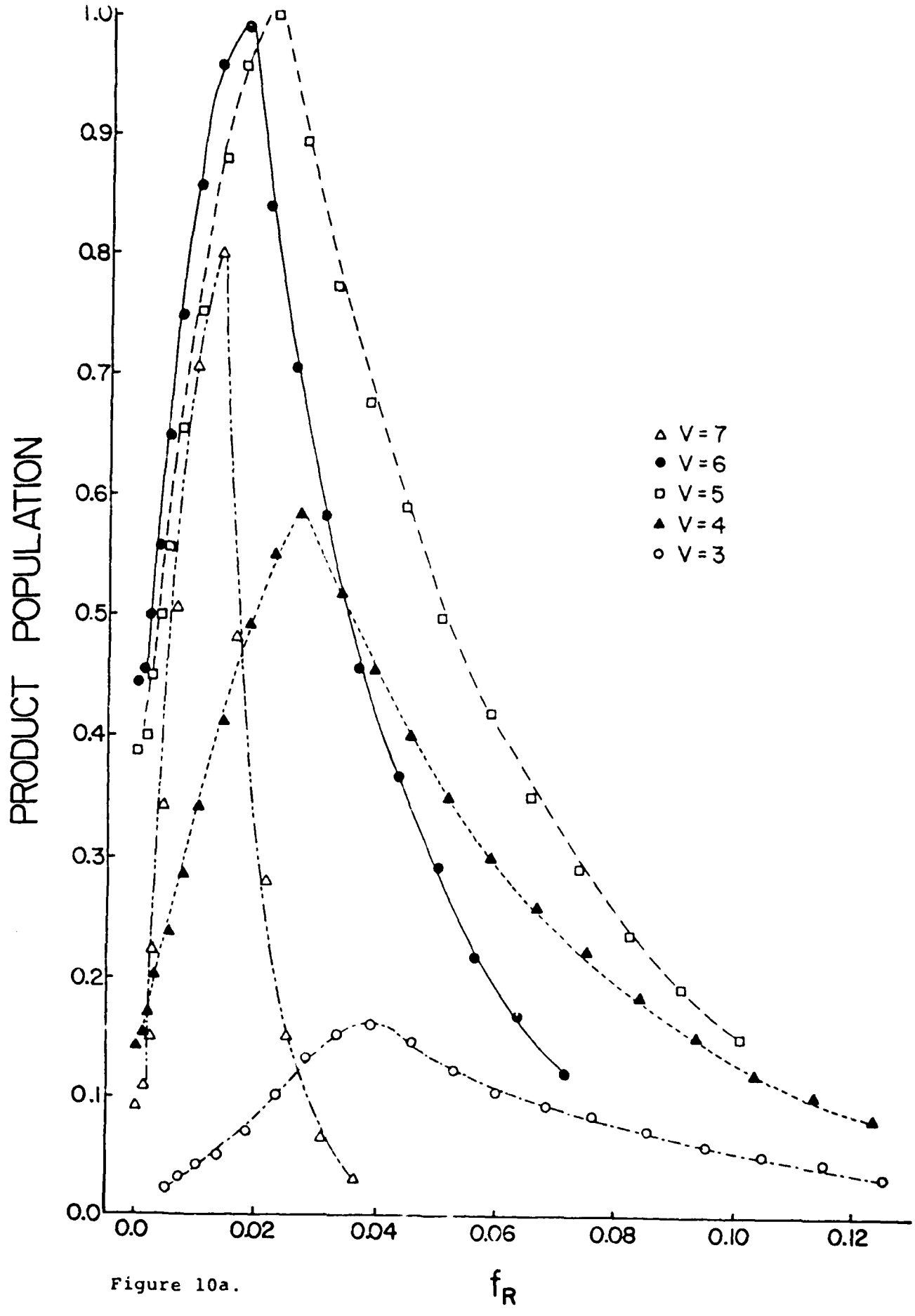
PRODUCT POPULATION
1.0
0.9
0.8
0.7
0.6
0.5
0.4
0.3
0.2
0.1
0.0
0.0
0.02
0.04
0.06
0.08
0.10
0.12
f_R
V = 7
V = 6
V = 5
V = 4
V = 3

Figure 10a.

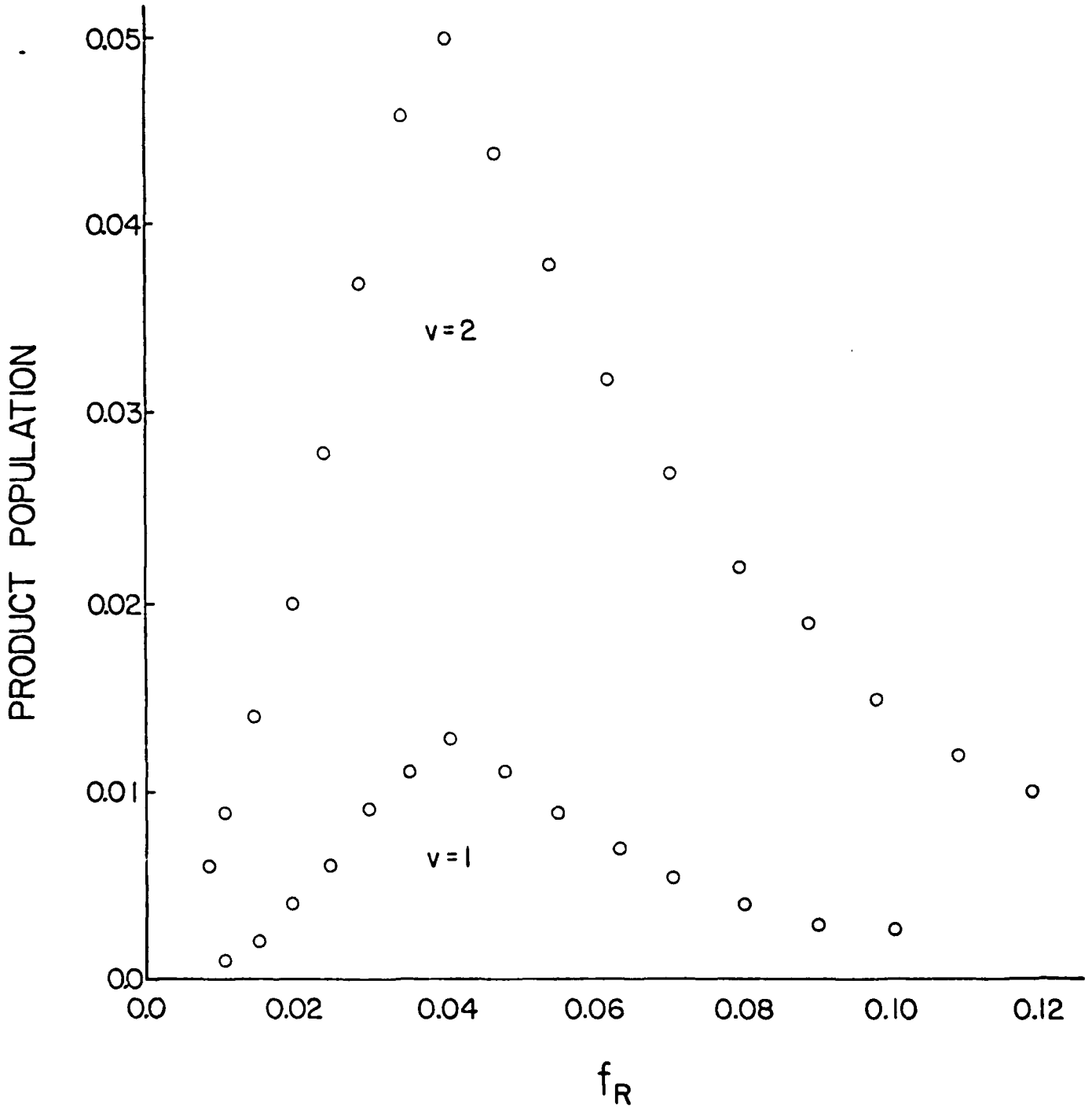
PRODUCT POPULATION
0.05
0.04
0.03
0.02
0.01
0.0
v=2
v=1
0.0
0.02
0.04
0.06
0.08
0.10
0.12
f_R

Figure 10b.